Research Square

Preprints are preliminary reports that have not undergone peer review.
They should not be considered conclusive, used to inform clinical practice,
or referenced by the media as validated information.

Effects of human umbilical cord mesenchymal stem cell (hUC-MSC)-derived exosomes on HIBD immunoinflammation in neonatal rats

Xiaoyun Xiong
West China Second University Hospital of Sichuan University
Ziyu Luo
Sichuan Stem Cell Bank & Sichuan Neo-Life Stem Cell Biotech Inc
Juan Chen
chenjuan2000@163.com
West China Second University Hospital of Sichuan University

Article

Keywords: Neonatal hypoxic-ischemic encephalopathy, Exosome, miRNA-146a-5p, Human umbilical cord mesenchymal stem cells

Posted Date: July 16th, 2026

DOI: https://doi.org/10.21203/rs.3.rs-9648687/v1

License: This work is licensed under a Creative Commons Attribution 4.0 International License.
Read Full License

Additional Declarations: No competing interests reported.

1.The title of the manuscript

Effects of human umbilical cord mesenchymal stem cell (hUC-MSC)-derived exosomes on hypoxic-ischemic brain damage (HIBD) immunoinflammation in neonatal rats

2.The full name and institutional addresses for all authors.

Xiaoyun Xiong[1,†], Ziyu Luo[2,†], Juan Chen[1,*]

[1] Key Laboratory of Birth Defects and Related Diseases of Women and Child (Sichuan University), Ministry of Education, West China Second University Hospital, Sichuan University, Sichuan Province, China.

[2] National and Local Joint Engineering Laboratory for Somatic Stem Cells, Sichuan Stem Cell Bank & Sichuan Neo-Life Stem Cell Biotech Inc., Chengdu, Sichuan Province, China.

[*] Corresponding author: Key Laboratory of Birth Defects and Related Diseases of Women and Child (Sichuan University), Ministry of Education, West China Second University Hospital, Sichuan University, Sichuan Province, China, Email address: chenjuan2000@163.com (Juan Chen).

[†] These authors contributed equally to this work.

3.Declarations

Ethics approval and consent to participate

This study was approved by the Ethics Committee of The West China Second Hospital Research Ethics Committee (Medical Research 2023 Ethics Approval No. (038)) and performed in accordance with

relevant guidelines and regulations. The data are anonymous and the requirement for informed consent was therefore waived by The West China Second Hospital Research Ethics Committee.

Consent to publish

Not applicable.

Data Availability Statement

All data supporting the findings of this study are available within the paper and its Supplementary Information.

The datasets generated and/or analysed during the current study are available in the [NCBI-Genbank-SRA] repository, [BioProject ACCESSION NUMBER: PRJNA1469413:015614BAC_50, SRA ACCESSION NUMBER: SRR38797903]

Competing Interests

The authors have no relevant financial or non-financial interests to disclose.

Funding

The authors declare that no funds, grants, or other support were received during the preparation of this manuscript.

Author Contributions

All authors contributed to the study's conception and design. Material preparation, data collection, and analysis were performed by Xiaoyun Xiong, Ziyu Luo, and Juan Chen, the first draft of the manuscript was written by Xiaoyun Xiong, and all authors commented on previous versions of the manuscript. All authors read and approved the final manuscript.

Acknowledgement

This thesis would not have been possible without the consistent and valuable reference materials that I received from my supervisor（Juan Chen）, whose insightful guidance and enthusiastic encouragement during the shaping of this thesis gain my deepest gratitude. and We also thank colleagues in the Department of Neonatology of West China Second Hospital for their help.

Effects of human umbilical cord mesenchymal stem cell (hUC-MSC)-derived exosomes on HIBD immunoinflammation in neonatal rats

Abstract

Objective

To investigate the effects of UC-MSCs-EXOS on immune inflammation of microglia caused by HIBD in neonatal rats. To explore the neuroinflammatory repair possibility and mechanism of UC-MSCs-EXOS transplantation in neonates with HIE.

Methods

In vitro experiments: The Oxygen and glucose deprivation (OGD) model was established. The growth and proliferation status of HAPI microglia was measured by CCK-8 method, the most suitable concentration of UC-MSCs--EXOS for the growth of HAPI cell line after OGD was identified. The expression of inflammatory genes in HAPI cell line after OGD were detected by q-PCR.

In vivo experiments:1. The HIBD model was established in vivo, the rats were divided into four groups: Sham operation control group (SHAM group), HIBD group, Exosomes intervention group (EXOS group), miRNA-146a-5p knockdown in EXOS intervention group (miRNA-146a-5p K/d group). the changes of M1 (CD16) and M2 (CD206) of rat microglia and the upstream signaling pathway of inflammatory factors were detected by Western blot after 72 hours of sampling. The gene expressions of M1 (CD16) and M2 (CD206) co-stained with microglia marker Ibal were detected by immunofluorescence. The expression of inflammation factors in rat brain tissue were detected by q-PCR. 2. Finally, the rats underwent a water maze test at 28 days to evaluate their spatial memory.

Results

Through in vitro experiments, we confirmed that the most suitable concentration of UC-MSCs-EXOS for the growth of HAPI cell line was 25 ng/ml. After OGD 6 hours, the expression of inflammatory factors IL-1β, IL-6 and TNF-α in HAPI cells were upregulated *($P<0.05$)*, whereas downregulated after 25 ng/ml EXOS co-culture for 24 h *($P<0.05$)*. Through in vitro experiments, we confirmed that UC-MSCs-EXOS could reduce microglial inflammation, in vivo experiments were continued to be explored.

In vivo experiments: after injection of 50 μg UC-MSCs-EXOS into the lateral ventricle

of rats, Western blot analysis showed that the expression of M1 proinflammatory marker (CD16) was decreased, while the expression of M2 anti-inflammatory marker (CD206) was increased *(P<0.05)*; Immunofluorescence results showed the same trend. the expression of inflammatory cytokines IL-1β, IL-6, TNF-α were downregulated (*P<0.05)*, the expressions of inflammatory factor upstream proteins IRAK and TRAF6 were downregulated after EXOS intervention (*P<0.05)*; After knockdown of miRNA-146a-5p with siRNA, various proteins and genes showed the opposite trend against unmodified UC-MSCs-EXOS intervention, Western blot analysis showed that the expression of M1 proinflammatory marker (CD16) was increased, while the expression of M2 anti-inflammatory marker (CD206) was decreased *(P<0.05)*; Immunofluorescence results showed the same trend. The expression of inflammatory cytokines IL-1β, IL-6, TNF-α were upregulated *(P<0.05)*, the expression of inflammatory factor upstream proteins IRAK and TRAF6 were upregulated after the intervention of knocked down exosomes *(P<0.05).* Water maze experiment: Compared with SHAM group, in the space exploration experiment, the number of platform crossings in HIBD group and miRNA-146a-5p K/d group were reduced *(P<0.05)*. Compared with HIBD group and miRNA-146a-5p K/d group, the number of platform crossings in EXOS group was increased, and the difference was statistically significant *(P<0.05).* EXOS intervention showed a promoting effect on long-term memory recovery in rats.

Conclusion

UC-MSCs-EXOS showed stem cell immunoregulation properties, down-regulating inflammatory factors IL-1β, IL-6 and TNF-α in HIBD rats and promoting microglia transformation from M1 proinflammatory phenotype to M2 phenotype. Finally presenting anti-inflammatory properties. which is accomplished by miRNA-146a-5p through IRAK and TRAF6 pathways.

Key words:

Neonatal hypoxic-ischemic encephalopathy; Exosome; miRNA-146a-5p; Human umbilical cord mesenchymal stem cells

Abbreviation table

Abbreviation	full name in English
HIBD	Hypoxic-Ischemic brain damage
HIE	Hypoxic-ischemic encephalopathy
NSCs	Neural Stem Cell
MSCs	Mesenchymal stem cells
UC-MSCs	Umbilical cord mesenchymal stem cells
EXOS	Exosomes
UC-MSCs-EXOS	Exosomes derived from umbilical cord mesenchymal stem cells
HI	Hypoxic ischemic
ASCs	Adult stem cells
OGD	Oxygen and glucose deprivation
HE	Hematoxylin and eosin
DMEM	Dulbecco's Minimum Essential Medium
PBS	Phosphate buffer saline
siRNA	Small interfering RNA
SHAM	Sham-operated control

1. Introduction

The brain injury resulting from hypoxic-ischemic encephalopathy (HIE) caused by perinatal asphyxia is called Hypoxic ischemic brain damage (HIBD) in neonates. The incidence of HIE in developed countries is approximately 1.5 per 1,000 live births, and HIE is a major cause of neonatal death [1; 2]. Hypoxic–ischemic injury (HI), based on severity and brain maturity, causes severe neurological sequelae in surviving infants, such as sensory-motor dysfunction, hearing and visual loss, learning disabilities, epilepsy, and cerebral palsy, and may even lead to neonatal death [3].

The pathogenesis of HIBD is complex. Currently, it is recognized that the innate immune response plays a key role in the pathogenesis of HIBD [4; 5]. The main mediator of the innate immune response to HIBD is microglia. Once activated upon injury, microglia release a large number of inflammatory factors, such as IL-6, IL-1β, and TNF-α [6; 7]; This immune response can aggravate the damage to the brain and nerves and, to a large extent, lead to subsequent neurodevelopmental defects [8].The microglial phenotype is also divided into M1 (pro-inflammatory phenotype) and M2 (anti-inflammatory phenotype). M1 microglial cells release inflammatory mediators and induce inflammation to produce neurotoxicity, while M2 microglial cells release anti-inflammatory mediators and induce anti-inflammatory and neuroprotective effects [9]. Multiple studies have shown that targeted microglia-mediated therapy has neuroprotective effects in several types of tissue injuries, suggesting that microglia may be a new therapeutic target for HIBD [10; 11; 12].

At present, there is no radical treatment measure for this disease. Hypothermia therapy is the only clinically approved intervention measure for full-term neonates diagnosed with moderate to severe HIBD [13]. It needs to start within 6 hours after birth, via either whole-body cooling or selective head cooling, for up to 72 hours, to reach the core body temperature of 34 ± 0.5 °C. Randomized controlled trials on hypothermia therapy have shown that among surviving infants aged 18-22 months, hypothermia therapy can reduce mortality, but has poor efficacy for severe HIBD [14; 15], Moreover, the application time window of hypothermia

therapy is relatively narrow. Hypothermia therapy needs to be performed within 6 hours after birth. Therefore, supplementary and/or alternative intervention measures need to be explored.

Recent studies have shown that stem cell therapy is a promising treatment option that is widely used in multi-system diseases. In the research of neonatal brain injury, stem cells exert a brain-protective effect due to their multiple functions. Compared with hypothermia therapy, it has no strict treatment time window, making it more clinically feasible. More and more animal experiments have shown the effectiveness of stem cell therapy, and there have also been beneficial results in human trials [16; 17]. Therefore, regenerative medicine methods represented by stem cell therapy have gradually been applied to injury repair and have demonstrated the ability to repair injuries in clinical trials.

Stem cells are pluripotent cells in tissues. They are mature cells that can self-renew and produce more stem cells or differentiate into specific tissues. Embryonic stem cells and Adult stem cells (ASCs) are the main types. Embryonic stem cells originate from blastocysts that are 3 to 5 days old and can produce any type of organ in the body. ASCs originate from specific tissues and possess the ability to self-renew and generate mature cells in a highly controlled micro-environment. ASCs has two characteristics. First, they can replicate themselves for a long time. Secondly, they can differentiate into mature cell types with characteristic morphology and special functions. Typically, ASCs differentiate into a type of intermediate cell called a precursor cell. Precursor cells are generally regarded as tissue-specific stem cells, dedicated to differentiating along specific cellular development pathways. New data indicate that ASCs can generate unrelated cell types. For example, bone marrow stem cells may be able to generate muscle cells or β-islet cells[18; 19]. ASCs include bone marine-derived monocytes, hematopoietic stem cells, pluripotent stem cells and Mesenchymal stem cells (MSCs), etc [17].

Neural Stem cells (NSCs) are self-renewing and pluripotent cells. It has the potent to differentiate into various cell lineages such as neurons and astrocytes [20]. However, studies have shown that the number of newly formed neurons is very small (about 5% of the transplanted cells differentiate into neurons), In addition, NSCs can be genetically modified before transplantation to overexpress neurotrophic factor-3 (NT-3), whose paracrine effects

promote neuronal differentiation. This method increases the proportion of neurons derived from NSCs to about 20% [21], However, the efficiency of NSCs transplantation and differentiation into neuronal cells is relatively low, and they mainly play a role in neural repair through paracrine methods.

MSCs, which exist in the tissues of adults or children, belong to ASCs and possess subpopulations of cells capable of differentiating into mesodermal lineages [22]; MSCs can promote tissue repair. The mechanisms include: 1) paracrine secretion involving protein/peptide and hormone secretion; 2) Transfer mitochondria through microvesicles; 3) Transfer exosomes or microvesicles containing RNA and other molecules . It has long been a consensus that the differentiation of adult stem cells is usually limited to tissues derived from their germ layer. However, some literature reports that the differentiation of MSCs can be in tissues of the mesoderm [23; 24; 25]. MSCs can be isolated from bone marrow, umbilical cord, placental tissue, adipose tissue, dental pulp, neurons, skin, breast milk, etc [26].

Compared with MSCs derived from adult tissues, umbilical cord mesenchymal stem cells from fetal accessory sources represented by UC-MSCs have many advantages such as abundant sources, easy extraction, short doubling time, low immunogenicity, and long survival time after transplantation [27; 28]. Preclinical studies have confirmed that chemokines secreted by UC-MSCs can promote excitatory synaptic connections and enhance neuronal survival [29], And there have been reports of Phase I and Phase II clinical trials related to UC-MSCs for indications including HIE, pulmonary diseases and post-hemorrhagic hydrocephalus [30; 31; 32].

For a long time, MSC transplantation has been regarded as possessing low immunogenicity and capable of crossing histocompatibility barriers. However, the latest research has confirmed that allogeneic donor transplantation of MSCs leads to immune rejection, suggesting that MSCs may not actually have immune privilege. The ability of local substitution and differentiation into multiple tissue types was considered in early studies to enable MSCs to exert therapeutic effects. However, an increasing number of studies have shown that the mechanism underlying MSC therapy may lie in the large number of active factors produced by MSCs. Since the transplanted cells cannot survive for a long time, these

bio-active factors play an important role in the regulation of biological processes.

Extracellular vesicles are lipid bilayer vesicles secreted by cells into the extracellular space. The three main subtypes of extracellular vesicles are microvesicles, exosomes (EXOS), and apoptotic bodies. Among them, exosomes are almost present in all biological body fluids. Exosomes, also known as intraluminal vesicles, are enclosed by a lipid bilayer membrane and exist in plasma, urine, saliva, bronchial fluid, cerebrospinal fluid, breast milk, serum, amniotic fluid, lymph fluid, bile and gastric acid [33], with a diameter of 40-100 nm and a density of 1.13-1.19 g/mL, they contains proteins, mRNA, miRNA and DNA [34]. EXOS plays a role in cellular information transmission by altering the characteristics of recipient cells. The main methods for preparing exosomes include: ultracentrifugation to separate exosomes, separation based on exosome size, and exosome precipitation[35]. Exosomes may have considerable advantages over cells in terms of manufacturing, storage, handling, product shelf life and potential as off-the-shelf biological products [36; 37].

Studies have shown that EXOS derived from MSCs can exhibit immune characteristics similar to their parent cells. Transplanting EXOS instead of intact mesenchymal stem cells is sufficient to exert therapeutic effects [38], Compared with cell therapy, exosome treatment has the advantage of higher safety, mainly due to their nanoscale size. Compared with MSCs with a diameter of 30-60 μm, nanoscale exosomes can effectively transfer to specific tissues after administration without accumulating in the pulmonary microvascular system, avoiding the possibility of pulmonary embolism caused by intravenously administered cells [39; 40; 41]. In recent years, UC-MSCS-derived exosomes have been widely used in the research of regenerative medicine due to their non-invasive collection methods, high proliferative capacity and low immunogenicity, such as neural repair of kidney injury and brain injury [42; 43; 44; 45].

Numerous studies have reported that exosomal miRNA-146a-5p alleviates inflammation by inhibiting the IRAK1/TRAF6 signaling pathway [46; 47; 48], miRNA-146a-5p can promote the anti-inflammatory properties of microglia and astrocytes. miRNA-146a-5p belongs to the miRNA-146a lineage. miRNA-146a-a is A key player in immunity and diseases. Studies have confirmed that the target protein of miRNA-146a is IRAK1/TRAF6[49], which participate in the NF-κB pathway involved in congenital

immune inflammation [50]. Activation of the NF-κB pathway is involved in the neuroinflammatory response after HIE [12; 51].

However, relevant reports on HIBD are currently relatively rare. Due to the lack of research data, the present study aims to establish a neonatal rats of HIBD, prepared EXOS from UC-MSCs, evaluate the effect of UC-MSCS-Exos on immune inflammation in neonatal rats with HIBD, and explore the possible mechanism. This study aims to provide theoretical support for the application of UC-MSCs-EXOS in the treatment of neonatal HIBD.

2. Results

2.1 Phenotypic characterization and differentiation potential of UC-MSCs

Flow cytometric immunophenotyping confirmed that the isolated cells were human umbilical cord mesenchymal stem cells (hUC-MSCs). These cells exhibited high expression of the typical MSC surface markers CD73 (95.56%), CD90 (99.13%), CD105 (97.24%), while showing minimal to no expression of hematopoietic lineage markers (CD34, CD45, CD11b, CD19) or the immunogenic marker HLA-DR (Figure 1). Furthermore, the cells were demonstrated to have multipotent differentiation capacity, successfully differentiating into osteogenic and adipogenic lineages as evidenced by Alizarin Red S and Oil Red O staining, respectively (Figure 2A, 2B). At about 3 weeks, obvious calcium mineralized nodules were formed in the P5 generation hUC-MSCs culture system, and the nodules were stained into scarlet/red-orange by Alizarin Red S (Figure 2A) and the lipid droplets that appeared during the lipid-inducing solution (red and transparent oil droplets could be seen in the cytoplasm of the cells by oil red O staining) (Figure 2B). Pre-transplantation cell viability was 69.17%.

2.2 Isolation and characterization of UC-MSC-derived exosomes

Exosomes were successfully isolated from conditioned medium of hUC-MSCs. Nanoparticle tracking analysis (NTA) revealed a average particle concentration of 3.5×10^{11} particles/mL with a peak size of 114 nm, fitting the expected size range for exosomes (40-200 nm). Western blot analysis confirmed the presence of exosome-specific positive markers (CD63, CD81, CD9, TSG101, Alix) and the absence of the negative marker Calnexin (Figure 3).

2.3 MicroRNA profiling of UC-MSC-EXOS

Microarray sequencing of UC-MSCs-EXOS was performed to profile their miRNA cargo. The results identified miRNA-146a-5p as one of the most highly abundant miRNAs, ranking among the top ten most abundant miRNAs in the exosomes (Figure 4). Given prior experimental evidence demonstrating that miRNA-146a-5p can promote microglial polarization toward an anti-inflammatory phenotype, we subsequently employed a knockdown strategy targeting miRNA-146a-5p. This approach was designed to further

investigate the specific contribution of this miRNA to the observed changes in microglial inflammatory phenotypes.

2.4 In vitro anti-inflammatory effects of UC-MSC-EXOS

Microarray sequencing of UC-MSCs-EXOS identified miRNA-146a-5p as one of the most highly expressed miRNAs (Figure 4). In vitro, a concentration of 25 ng/ml UC-MSCs-EXOS was found optimal for promoting the proliferation of HAPI microglial cells post-oxygen and glucose deprivation (OGD) *($P<0.001$)* (Figure 5). qPCR analysis demonstrated that UC-MSCs-EXOS treatment significantly downregulated the expression of pro-inflammatory cytokines (IL-6, IL-1β, TNF-α) in OGD-treated HAPI cells *($P<0.05$)* (Figure 6).

2.5 In vivo neuroprotective efficacy of UC-MSC-EXOS in neonatal HIBD model

A neonatal hypoxic-ischemic brain damage (HIBD) rat model was successfully established, as confirmed by histopathological (HE staining) and morphological (TTC staining) analyses, which showed cellular disarray, necrosis, and significant infarction in the HIBD group compared with the SHAM group (Figures 7 & 8). Intracerebroventricular administration of UC-MSCs-EXOS (50 μg) 72 hours post-HIBD significantly reduced infarct volume *($P<0.001$)* (Figure 8). Furthermore, EXOS treatment modulated microglial polarization, decreasing the M1 marker (CD16) and increasing the M2 marker (CD206) at the protein level as shown by Western blot and immunofluorescence data *($P<0.05$)* (Figures 9 & 11). This trend was accompanied by a significant reduction in brain tissue levels of IL-6, IL-1β, and TNF-α *($P<0.05$)* (Figure 10). Mechanistically, EXOS treatment downregulated key proteins (IRAK1, TRAF6) in the pro-inflammatory signaling pathway *($P<0.05$)* (Figure 12).

2.6 Role of miRNA-146a-5p in mediating the effects of UC-MSC-EXOS

The functional importance of miRNA-146a-5p was investigated using siRNA knockdown (KD) in UC-MSCs prior to exosome collection (Figure 13). Compared to treatment with normal EXOS, administration of miRNA-146a-5p-KD EXOS failed to suppress post-HIBD inflammation. Specifically, the miRNA-146a-5p-KD-EXOS group showed higher expression of pro-inflammatory cytokines (IL-6, IL-1β, TNF-α) *($P<0.05$)* (Figure 14), an

increased M1/M2 microglial ratio *(P<0.05)* (Figure 15A, 15B), and elevated levels of IRAK1 and TRAF6 proteins *(P<0.05)* (Figure 16) relative to the normal EXOS group.

2.7 Functional recovery assessed by Morris water maze test

Behavioral assessment using the Morris water maze over 5 days showed that HIBD rats exhibited significantly longer escape latencies than SHAM controls. UC-MSCs-EXOS treatment markedly improved spatial learning and memory, as demonstrated by significantly shorter escape latencies (days 1-5, *P<0.05*) and a greater number of platform crossings in the probe trial compared with the HIBD and miRNA-146a-5p-KD EXOS groups (*P<0.05*). The performance of the EXOS-treated group was comparable to that of the SHAM group in the probe trial (*P>0.05*) (Figure 17).

3. Discussion

In the literature reports on the pathogenesis of neonatal HIBD, immune inflammation is an important pathogenesis of HIBD. The activation of microglia causes oxidative stress and secretes pro-inflammatory cytokines (IL-6, TNF-α, IL-1α and IL-1β) and IFN-γ[53]. The in vitro experimental results in this study indicated that OGD activated the inflammatory responses mediated by microglia, and the expressions levels of IL-6, TNF-α, IL-1α and IL-1β were upregulated after OGD. In the in vivo experiments, during the acute phase of HIBD, the secretion of pro-inflammatory cytokines IL-6, TNF-α and IL-1β by microglia increased, inducing secondary cytotoxicity. All these findings are consistent with the previous reports.

Studies have proved that reducing microglia-mediated neuroinflammation is beneficial during the recovery period of HIBD [54]. Stem cell therapy is a promising treatment option, clinical trials on the transplantation of MSCs for bronchopulmonary dysplasia and intraventricular hemorrhage have been reported [32; 55; 56]. However, the mechanism of cure is still not completely clear. For a long time, the notion that MSCs act through homing and differentiation into tissue cells to replace damaged cells has been largely disproven [57]. The role of stem cell therapy in directly replacing tissues is limited, as more than 99% of transplanted MSCs are trapped in the pulmonary vascular system,

which hinders the therapeutic effect [41]. Preclinical studies have shown that local or systemic transplanted MSCs used for repairing various injuries by secreting soluble paracrine molecules, exerting anti-inflammatory, anti-apoptotic, antioxidant, anti-fibrotic, antibacterial and permeability stabilizing effects [58; 59]. In addition to bioactive factors, MSCs can also secrete extracellular vesicles such as exosomes. These vesicles transmit signals to host cells and modulate cell functions, thereby exert repair effects [60].

EXOS contains microRNAs (miRNAs), miRNAs are short non-coding RNAs that inhibit gene expression by directly binding to the mRNA of target genes[35; 42].Research reports have indicated that EXOS play a significant role in the inter-cellular transfer of miRNAs, delivering biologically active miRNAs to adjacent and distant cells through interstitial fluid and circulation [61; 62]. For example, the miR-204-mediated IL-6/IL-6R/Stat3 signaling reprograms pro-inflammatory M1 macrophages into an immunosuppression phenotype, miR-182 alleviates myocardial ischemia-reperfusion injury by regulating the polarization of macrophages. These studies explored the potential therapeutic effect of hUC-MSC-EXOS in improving HIBD injury.

A large number of studies have confirmed that EXOS derived from MSCs can play a potent protective role in HIBD, such as regulating the NF-κB signaling pathway to induce anti-inflammatory properties in astrocytes [63]. Furthermore, it is known that miR-7116-5p negatively regulates protein polyubiquitination, thereby promoting angiogenesis and neurogenesis [64]. Although it is difficult to completely rule out the influence of other miRNAs on microglia in this study, the investigated miRNA is regarded as a key functional element. miR-146a-5p is a well-known anti-inflammatory molecule and plays a key role in inflammatory diseases [65; 66; 67]. Receptor proteins IRAK1 and TRAF6 are abundant in the cytoplasm and nucleus of various cell types [68]. They are mainly involved in the pathways initiated by Toll-like receptors (TLRS), leading to the expression of pro-inflammatory mediators [69]. The overexpression of IRAK1 and TRAF6 can activate NF-κB. miR-146a-5p bonds to the mRNA encoding IRAK1 and TRAF6 to down-regulate the inflammatory response[70; 71]. However, in this study, only the receptor proteins IRAK1 and TRAF6 were examined. In our in vivo experiments, injection with unmodified EXOS after HIBD, downregulated the expressions of IRAK1 and TRAF6, whereas their

expressions were upregulated after knockdown of miRNA-146a-5p. It was confirmed that the target proteins of miRNA-146a-5p are IRAK1 and TRAF6, and they are involved in the regulation of the HIBD inflammatory response. However, the expression of other proteins in the TLR/NF-κB signaling pathway still needs to be verified in subsequent experiments.

Microglia are key regulatory factors of the inflammatory response in the central nervous system. Traditionally, they can be classified as neurotoxic (M1 phenotype microglia) or neuroprotective (M2 phenotype microglia)[72]. Upon activation, microglia polarize toward the pro-inflammatory M1 phenotype, with significantly increased secretion of inflammatory factors TNF-α, IL-1β and IL-6[73]. M1 phenotype markers include CD16, CD32 and CD86. While the M2 marker is CD206[74].

The results of this study indicated that in vivo administration of 50 μg EXOS into the lateral ventricle of rats downregulated the expression of the pro-inflammatory M1 phenotype marker CD16, upregulated the expression of the anti-inflammatory M2 phenotype M2 marker CD206, as determined by Western blot. Immunofluorescence shows the same trend, the expressions of inflammatory factors IL-1β, IL-6 and TNF-α were downregulated, and the upstream proteins of inflammatory factors IRAK and TRAF6 were downregulated after transplantation of unmodified EXOS. When using siRNA to knockdown miRNA-146a-5p, the gene expression showed an opposite trend compared with treatment using intact EXOS. According to Western blot results, the expression of the pro-inflammatory M1 phenotype marker CD16 was upregulated, and the expression of the anti-inflammatory M2 phenotype marker CD206 was downregulated. Immunofluorescence shows the same trend, the expressions of inflammatory factors IL-1β, IL-6, and TNF-α were upregulated, and the upstream proteins of inflammatory factors IRAK and TRAF6 were upregulated following treatment with miRNA-146a-5p-knockdown EXOS. These results indicated that EXOS transplantation in neonatal rats downregulated the expression of the inflammatory M1 phenotype marker CD16, thereby promoting microglial polarization towards M2 phenotype and upregulating of M2 marker CD206. However, after knockdown of miRNA-146a-5p with siRNA, the expression of M1 marker CD16) in microglia was upregulated, and M1 polarization

occurred. The results of this study indicate that in the HIBD rat model, administration of UC-MSC-EXOS to the lateral ventricle 24 hours after HI enables the EXOS to cross the blood-brain barrier and enter the ischemic injury site, and then be absorbed by local microglia. Among them, miR-146a-5p derived from UC-MSC-EXOS could inhibit the M1 polarization mediated by the IRAK1/TRAF6 signaling pathway and the subsequent production of potent pro-inflammatory cytokines, ultimately alleviating the degree of tissue edema, cell death and ischemic injury induced by HI.

In addition to needing further studies on the therapeutic potential of free miR-146a-5p in HIBD and inflammatory diseases, the present results also raised many interesting theoretical questions. For example, it is currently unclear whether UC-MSCs-EXOS is involved in repairing neuronal injury. Furthermore, will other miRNAs affect the microglial function after HIBD? Does UC-MSCs-EXOS also affect the functions of other cell types of HIBD such as neurons, astrocytes and/or oligodendrocytes? Finally, the mechanisms by which UC-MSCs-EXOS ameliorate HIBD, as well as the issues related to immune rejection and the safety of cell transplantation, all require in-depth investigation and validation in future studies.

4. Conclusion

UC-MSCs-EXOS can promote the transition of microglia from the M1 pro-inflammatory phenotype to the M2 phenotype and downregulate the expression of inflammatory factors IL-1β, IL-6, and TNF-α in HIBD rats. This process may be mediated by miRNA-146a-5p through the pathways of IRAK and TRAF6. In conclusion, UC-MSCs-Exos or miR-146a-5p may promote microglial polarization toward to an anti-inflammatory effects, and thus represent a novel therapeutic strategy for HIBD, which needs further investigation.

5. Materials and methods

5.1 Materials

5.1.1 Main reagents

Reagent	Source
Microglia of HAPI rats	Haiyaji Biotechnology Co., LTD
Anti-TRAF6 antibody	Abcam
Anti-Iba1 antibody	Abcam
Anti-Myelin Basic Protein antibody	Abcam
Anti-GFAP antibody	Abcam
Goat Anti-Rabbit IgG H&L	Abcam
Goat Anti-Mouse IgG H&L	Abcam
InstantBlue Coomassie Protein Stain (ISB1L)	Abcam
Anti-IRAK-1 antibody	Abcam
Anti-Mannose Receptor antibody	Abcam
Anti-NeuN antibody [EPR12763] - Neuronal Marker	Abcam
Anti-CD9 antibody	ZENBIO
Anti-ALIX antibody	ZENBIO
Anti-TSG101 antibody	ZENBIO
Anti-CD63 antibody	ZENBIO
Anti-CD81 antibody	ZENBIO
Anti-Calnexin antibody	ZENBIO
Anti-actin antibody	ZENBIO
RIPA Lysis Buffer	Xinsaimei
Precision Plus Protein Dual Color Standards	Bio-rad
Anti-CD16 antibody	Abcam
DAPI Dyeing reagent (ready-to-use type)	Seville

Fluorescent mounting agent	Nakasugi Golden Bridge
Precision Plus Protein Dual Color Standards	Bio-rad
Protease inhibitors (excluding EDTA)	Roche
WesternBlot The "Fast Three Musketeers" (Rapid Electrophoresis solution, Rapid electrotransfer solution, Protein-free rapid Blocking Solution)	Pulley
Trizol reagent	Thermos
PrimeScript RT kit	Takara
SYBR Green PCR	Bio-rad
EXO-FECT Transfection kit	SBI
Bicinchoninic Acid Protein Assay Kit	Beyotime Biotechnology

5.1.2 Main experimental instruments

Instrument	Manufacturer
Thermo KS12 Clean Bench	Thermo, USA
Laser confocal microscope	OLYMPUS, Japan
Fluorescence quantitative PCR instrument	Bio-rad
Laboratory pure water instrument	Merk Millipore, USA
Microplate reade	Bio-rad
The United States Constant temperature water bath box	Heto-Hoten, Denmark
CO_2 incubator	Thermo, USA
Wb Western blotting instrument	Bio-rad
Vortex instrument	IKA, Germany
X71 inverted phase contrast fluorescence microscope	Olympus, Japan

benchtop centrifuge SORVALLR LEGEND RM	Thermo, USA
water-bath electric heating constant temperature incubator	Shanghai Yuejin Medical Device Factory
Temperature-controlled benchtop centrifuge SORVALLR LEGEND	Thermo, USA
Micropipette	Eppendorf, Germany

5.2 Experimental animals and cells

5.2.1 Cell culture and OGD model establishment

HAPI cells were purchased from Shanghai Yaji Biotechnology Co, Ltd. The HAPI cell line was cultured in DMEM (Dulbecco's Minimum Essential Medium; Dalberk's essential basic medium) (2%B27, 0.5% glutamine and 97.5%neurobasal plus). Inoculate 1×10^6 cells per well into each 6-well plate.The OGD model was performed using DMEM glucose-free medium in a three-gas incubator under anoxic conditions (1%O_2, 5% CO_2 and 94% N_2) for 6 hours.

5.2.2 Experimental grouping and treatment

Cells were divided into the SHAM group, the OGD group and the EXOS group. The SHAM group received no treatment. The OGD group was given DMEM glucose-free medium. In the EXOS group, after 6 hours of OGD in HAPI cells, 25 ng/ml EXOS was added and co-cultured for 24 hours before collecting the cells. After 24 hours, RNA was extracted from cells in each group for quantitative real-time PCR (qPCR).

5.2.3 Cell viability assay (CCK-8)

The cell viability of HAPI microglia was determined. HAPI cells were inoculated into 96-well plates, and 10 μl of CCK-8 solution was added to each well. Then incubate the plate for 90 minutes. The absorbance was measured at 450 nm using a microplate analyzer.

5.3 Animal experiments

The experimental animals (SD rats, 7 days old, each weighing 20-30g) were purchased from the Animal Experiment Center of Sichuan University (Chengdu, China). They were fed a standard laboratory diet, with food and water obtained at will. They were kept in a controlled room at a temperature of 22±1°C and a humidity of 65-70% for 12 hours in a light and dark cycle. All the guidelines for the use of experimental animals are implemented in accordance with the guidelines of the National Institutes of Health of the United States and have been approved by the Ethics Committee of Sichuan University.

5.3.1 Animal experimental groups

7-day-old SD rats (240 rats) were divided into four groups: SHAM operation control group (SHAM group), hypoxia-ischemic brain injury group (HIBD group), exosome treatment group (EXOS group), and knockdown exosome (miRNA-146a-5p k/d) treatment group , hereinafter referred to as the miRNA-146a k/d group.

5.3.2 Establishment of HIBD rat model

All experiments were designed and implemented in accordance with the guidance of the Research Animal Nursing Committee of Sichuan University. Pregnant rats were purchased from Chengdu Dashuo Experimental Animal Center. HIBD was induced by ligation of the right common carotid artery, followed by hypoxia (8% O_2, 92% N_2) in the hypoxia chamber for 2 hours. After modeling, the animals were sacrificed within 24 hours for Hematoxylin and eosin (HE) staining to evaluate the cerebral infarction status, in order to assess whether the HIBD model establishment was successful.

5.3.3 Drug treatment for each group

In the EXOS group, 50 μg EXOS was injected into the lateral ventricle after 2 hours of HI. In the miRNA-146a k/d group, 50 μg EXOS with miRNA-146a-5p knocked down was given at 2 hours of HI. The sham operation group and the HIBD group were not given solvents.

5.4 Experimental methods

5.4.1 Identification of UC-MSCs

UC-MSCs cells were Centrifuged at 300×g, for 5 minutes, discard the supernatant, and add a certain amount of PBS (Phosphate buffer saline); Wash with phosphate buffer and resuspend the cells; Take 100 μl of cells into a flow cytometer tube; After adding the corresponding antibodies and mixing well, incubate at room temperature in the dark for 15 minutes. Wash the cells with PBS, Centrifuge at 300×g, for 5 minutes, discard the supernatant, add PBS to resuspend the cells, and test on the machine.

5.4.2 Isolation and characterization of UC-MSC-EXOS

The UC-MSC-EXOS were obtained from cell culture chamber. The UC-MSC-EXOS at passage 5 were seeded into cell culture flasks (Corning) containing DMEM-F12 supplemented with 5% Platelet lysate for UC-MSC-EXOS isolation. when the cells reached around 80% confluence, the medium was replaced with conditioned medium, and the supernatant was collected after 2-3 days. UC-MSC-EXOS were isolated from the conditioned medium by standard ultracentrifugation methods as described previously[52]. a series of centrifugations were done to remove cellular components, cellular debris, and protein contaminants.

Protein and RNA analyses were conducted on the obtained UC-MSC-EXOS. Before use, all UC-MSC-EXOS samples underwent analyses for particle concentration and size using nanoparticle tracking analysis (Particle-Metrix ZetaVIEW). A BCA kit (Beyotime Biotechnology) was used to determine protein concentration in UC-MSC-EXOS preparations, and western blotting was used to assess UC-MSC-EXOS markers CD9, CD63, CD81, Alix, TSG101, Calnexin (ZENBIO). Subsequently, the samples were adjusted to the desired working concentrations for cells and animal applications.

5.4.3 HE staining

Twenty-four hours after modeling, samples were collected from the cut ends, fixed with 4% paraformaldehyde, dehydrated in graded alcohols, cleared in xylene, and embedded in

paraffin. Then cut the sample into 5 μm slices and dry them. Dewaxing the xylene, rehydrating it with alcohol and dyeing it. The pathological changes of the sections were observed using an optical microscope.

5.4.4 Infarct area determination

After 72 hours of modeling, the brain was harvested after decapitation, placed in a −20 °C refrigerator for 10–20 minutes, and then sectioned. Each brain was cut into four pieces,with a slice thickness of 2 millimeters. Then, the slices were incubated with 2% TTC at 37°C for 20 minutes, fixed with 4% paraformaldehyde and photographed. The total brain volume was calculated using Image-Pro Plus 6.0 software. The percentage of infarction was calculated as infarct volume divided by total brain volume.

5.4.5 Western blotting

At 72 hours after modeling, truncated samples were collected. The tissues were lysed using RIPA buffer (KeyGEN BioTECH), and then protein quantification was performed using the Bradford protein detection kit (KeyGEN BioTECH). In short, the lysate was treated with SDS-PAGE and transferred onto the PVDF membrane (Millipore). According to the requirements of each experiment,the membrane was incubated overnight with the primary antibody specific to the following protein at 4°C: CD16 (diluted at 1:1000; Abcam), CD206 (diluted at 1:1000, Abcam), TRAF6 (diluted at 1:1000, Abcam), IRAK1 (diluted at 1:1000; The next day, the membrane was incubated with the corresponding secondary antibody. Finally, after PBS washing, the protein spots were visualized using the chemiluminescence kit (Thermo Scientific). The internal reference protein GAPDH was selected as the internal control. Each experiment is in triplicate.

Membranes were trimmed to the approximate molecular weight of the target protein before exposure, a routine practice to optimize signal detection. Due to this pre-exposure trimming, full-length membrane images are not available. The images presented in the main figures represent the entire remaining membrane strips after trimming. All key experiments were repeated independently at least three times, and the most complete raw images are provided in the Supplementary materials.

5.4.6 Immunofluorescence

At 72 hours after modeling, samples were harvested after decapitation for immunofluorescence staining. The brain was fixed with paraformaldehyde, dehydrated with sucrose, embedded in OCT, frozen in liquid nitrogen, and stored at -80°C for subsequent sections. The sections were immersed in phosphate buffered saline (PBS) for 10 minutes to remove OCT, and the Triton X-100 was used to penetrate the membrane. The slices were sealed with bovine serum for 1 hour. Next, 150 μl of diluted CD16 and CD206 antibodies (1:200) were added, and the sections were incubated. The sections were then washed with PBS, and the secondary antibody was added. Finally, the sections were stained with DAPI, washed with PBS, mounted with anti-fade mounting solution, and coverslipped. The sections were observed and photographed under a fluorescence microscope.

5.4.7 Real-time PCR

Total RNA was extracted from HAPI cells or truncated rat brain tissue using Trizol reagent (Thermo Scientific), Reverse transcription was performed using the PrimeScript RT kit (Takara Bio Inc). Real-time PCR was performed using SYBR Green PCR premix (Bio-rad) and the Applied Biosystems 7500 Fast Real-time PCR system (Applied Biosystems). Shenggong provided the sequences of all primers.

Gene	Forward primer (5'-3')	Reverse primer (5'-3')
IL-6	ACTTCCATCCAGTTGCCTTCTTGG	TTAAGCCTCCGACTTGTGAAGTGG
TNF-α	GCGACGTGGAACTGGCAGAAG	GCCACAAGCAGGAATGAGAAGAGG
IL-1β	CTTCCATCCAGTTGCCTTCTTGG	TGCTCATGTCCTCATCCTGGAAGG

5.4.8 Microarray analysis

The miRNA profiles of total RNA in hUC-MSC-EXOS (n = 3) was analyzed by small RNA

deep sequencing (Illumina). Library preparation and miRNA sequencing were carried out by Ribobio (Guangzhou, China). In brief, total RNA samples were fractionated, and only small Rnas (with a length of 18-30 nucleotides) were used for library preparation. After PCR amplification, sequencing was performed.

5.4.9 Knockdown of miR-146a-5p via lentiviral vector transduction

Lentiviruses expressing miR-146a-5p inhibitors were used to infect and transduce hUC-MSCs at 200 particles/cells. The transduction was performed in 24-well plates using DMEM (HyClone). The content of miR-146a-5p in hUC-MSC-EXOS was evaluated by q-PCR to confirm successful transduction. No-load siRNA lentivirus was used as the control. The sequence of miRNA-146a-5p were listed below:

FORWARD: CGCGTGAGAACTGAATTCCA

REVERSE: AGTGCAGGGTCCGAGGTATT

5.4.10 Morris water maze test

On day of 28, the Morris water maze experiment was conducted in rats. Rats were tested 40 times per day for 6 consecutive days, with each trial lasting 5 seconds. The escape latency (time to find the platform) was recorded. On the sixth day, the platform was removed, all the animals were allowed to swim freely in the maze to test spatial memory. the time spent and number of entries into the target area (where the platform had been located) of each rat were recorded for spatial memory assessment.

5.5 Animal Euthanasia Procedure

All animal procedures in this study were approved by the Animal Care and Use Committee of Sichuan University and were performed in strict accordance with relevant ethical guidelines. At the designated time points (24 h, 72 h post-modeling, and after the 28-day Morris water maze test), animals were deeply anesthetized by isoflurane inhalation (induction at 4%, maintenance at 2–3% in 100% oxygen at a flow rate of 1 L/min). After the animals had lost consciousness completely, exhibited no pain reflexes, and presented shallow respiration, euthanasia was performed by decapitation or transcardial perfusion with fixative

for brain tissue collection. Euthanasia was conducted by trained personnel to minimize animal suffering. All efforts were made to reduce the number of animals used and their distress.

5.6 Statistical analysis

Data were processed using SPSS 16.0 statistical software. The experimental data were all expressed as mean ± standard deviation (x±s). One-way ANOVA was used for single set of experimental data, and Repeated-measures ANOVA was used for comparison among multiple groups with repeated measures. $P<0.05$ was considered statistically significant.

6.Figures

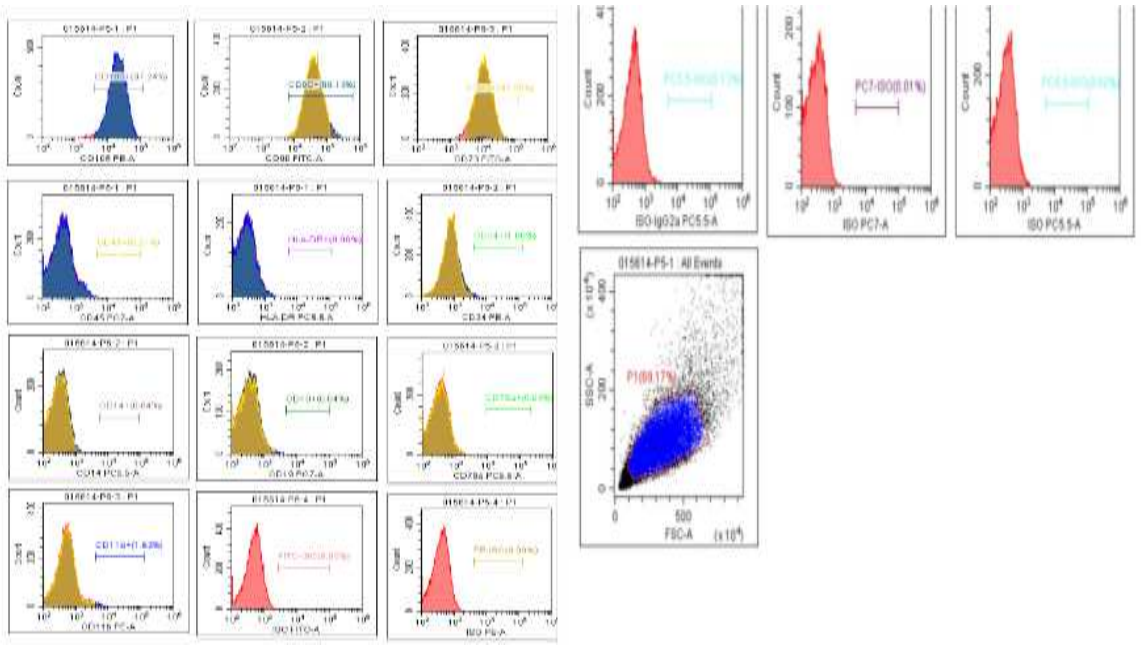


Figure1. Flow cytometry results of UC-MSCs surface antigens. UC-MSCs were analyzed by flow cytometry for expression of mesenchymal stem cell markers (CD73, CD90, CD105), hematopoietic lineage markers (CD34, CD45, CD11b, CD19), and the immunogenic marker HLA-DR

2A **2B**

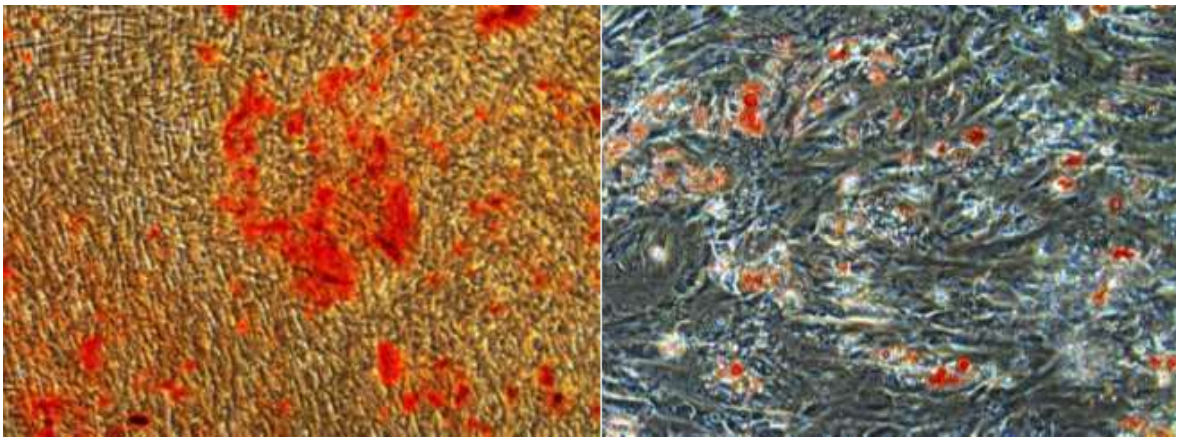


Figure2. Results of UC-MSCs induction in vitro. (A) osteogenic differentiation of UC-MSCs demonstrated by Alizarin Red S staining showing dense opaque red-orange precipitates (calcium nodules). (B) Adipogenic differentiation of UC-MSCs demonstrated by Oil Red O staining showing red transparent oil droplets in the cytoplasm.

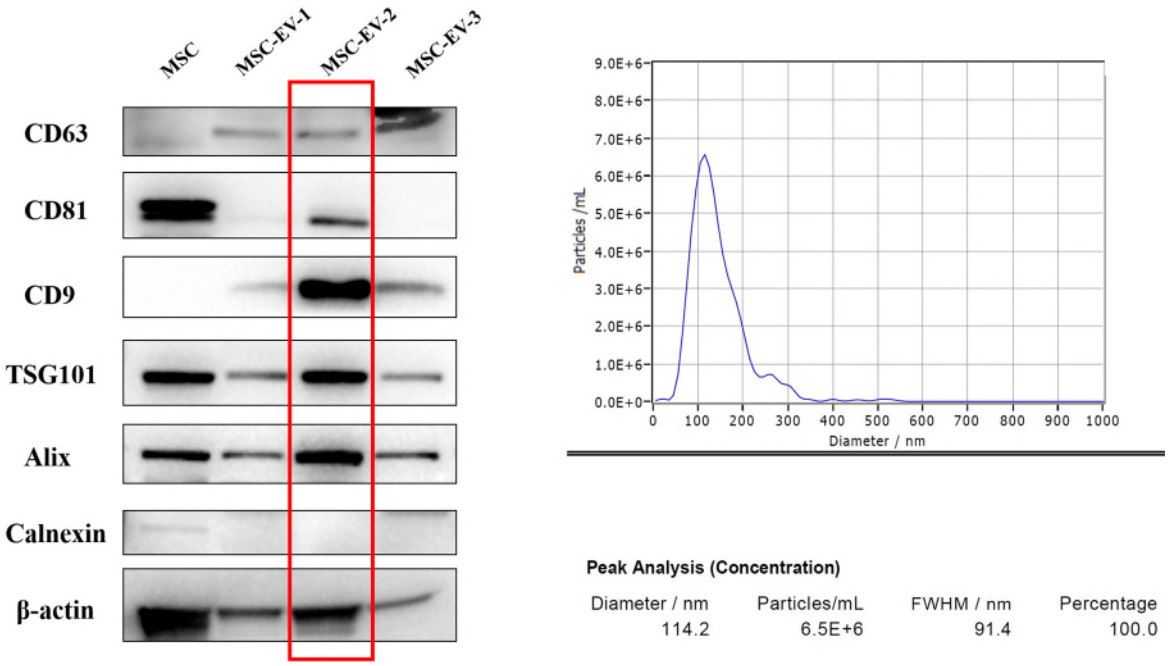


Figure 3. Identification of UC-MSC-EXOS. Representative nanoparticle tracking analysis showing exosome size distribution with peak at 114 nm. Representative western blot analysis confirming expression of exosome markers CD63, CD81, CD9, TSG101, and Alix, with absence of the negative marker Calnexin. The grouping of blots cropped from different parts of the different blots and from different fields. Exosomes utilized in the present study correspond to the MSC-EV-2 group illustrated herein (within the red box).

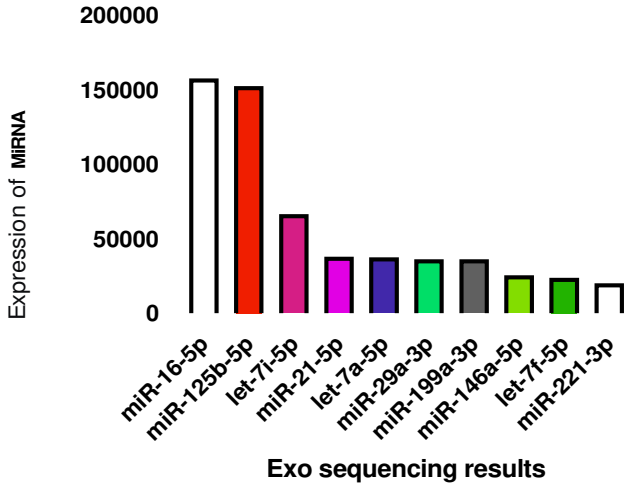
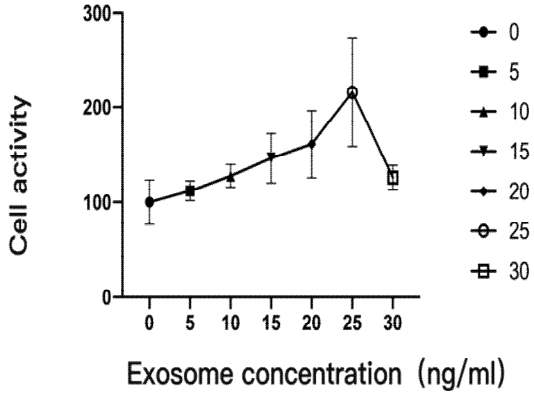


Figure 4. Top 10 miRNAs measured by UC-MSC-EXOS microarray. miRNA microarray analysis showing the ten most highly expressed miRNAs in UC-MSC-EXOS, with miRNA-146a-5p among the top-ranked miRNAs.



Effects of different exosome concentrations on HAPI cell viability after OGD

Figure 5. Effects of different concentrations of exosomes on the proliferation of HAPI cell lines. HAPI microglia were subjected to OGD treatment and then co-cultured with indicated concentrations of UC-MSC-EXOS. Cell viability was assessed by CCK-8 assay. Data are presented as mean ± SD, n=6, *$p < 0.05$、**$p < 0.01$、***$p < 0.001$.

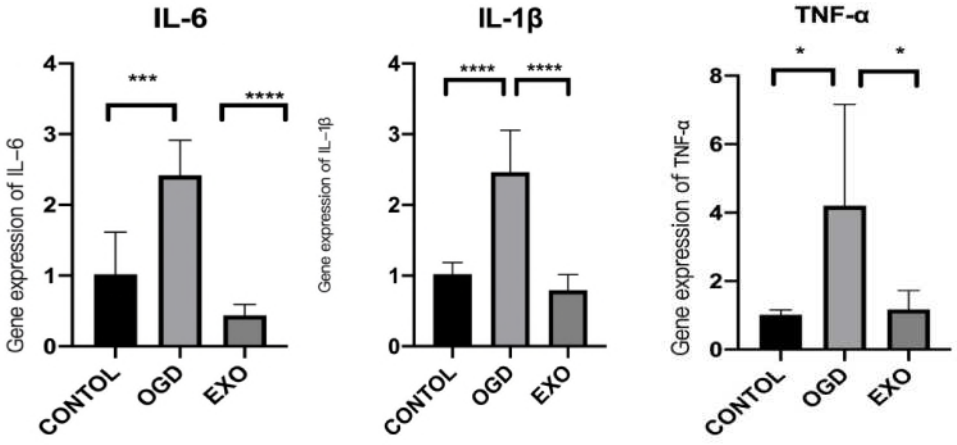


Figure 6. Inflammatory factor expression after OGD and exosome co-culture. HAPI cells were subjected to OGD treatment for 6 h followed by co-cultured with EXOS for 24 h. mRNA expression levels of IL-6, IL-1β, and TNF-α were measured by qPCR. Data are presented as mean ± SD, n = 6 from three independent experiments. *$p < 0.05$、**$p < 0.01$、***$p < 0.001$.

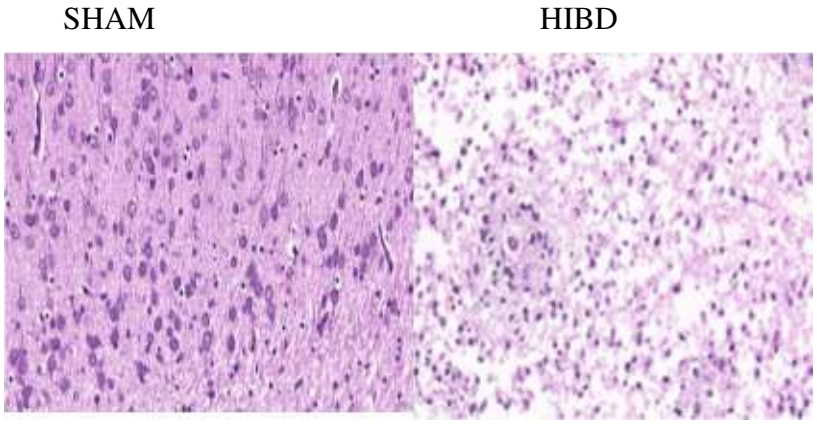


Figure 7. Pathological changes of HE-stained brain tissue 24 h after modeling (50× magnification). Representative HE-stained brain sections from SHAM and HIBD groups showing normal cellular architecture in SHAM group versus cellular disarray and nuclear condensation in HIBD group.

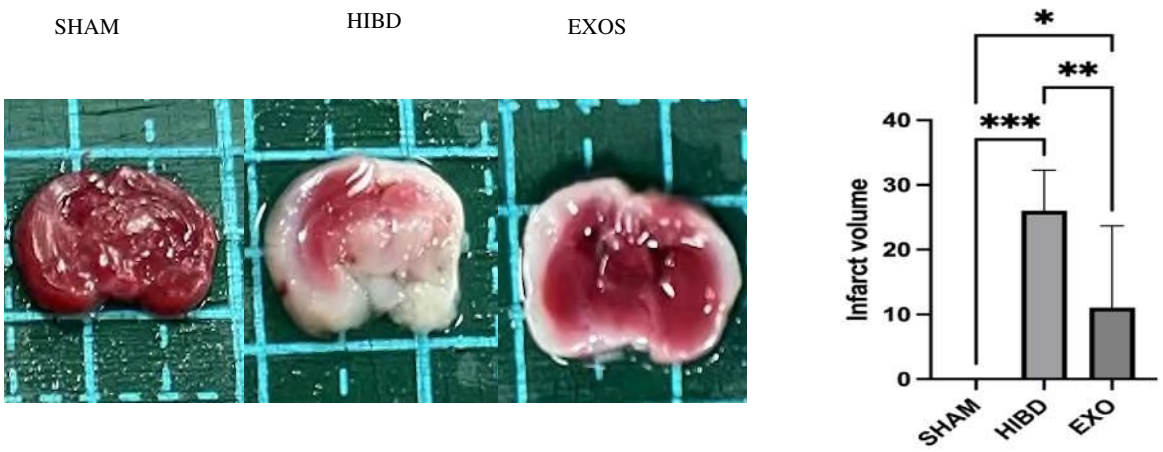


Figure 8. TTC staining and infarct size statistics of rat brain tissue 72 h after HI. Representative TTC-stained brain sections from SHAM, HIBD, and EXOS groups. White areas indicate infarcted tissue. Quantitative analysis of infarct volume expressed as percentage of total brain volume. Data are presented as mean ± SD, n = 3. $*p < 0.05$、$**p < 0.01$、$***p < 0.001$

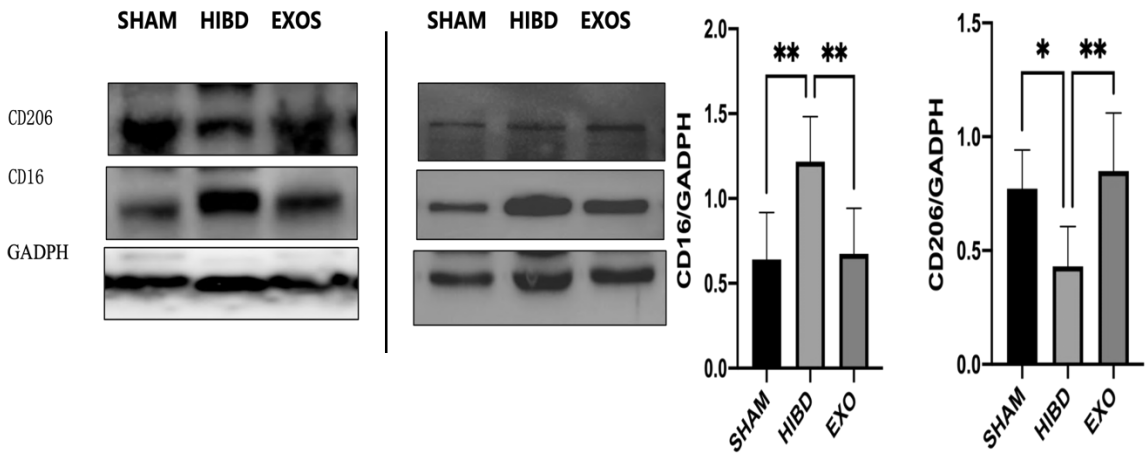


Figure 9. Expression of M1 (CD16) and M2 (CD206) in microglia after exosome transplantation in rats. Western blot analysis of CD16 and CD206 protein expression in brain tissue from SHAM, HIBD, and EXOS groups 72 h after EXOS administration. Data are presented as mean ± SD, n = 6. Black lines separate the two independent replicate blot shown in the same panel.*$p < 0.05$、**$p < 0.01$、***$p < 0.001$.

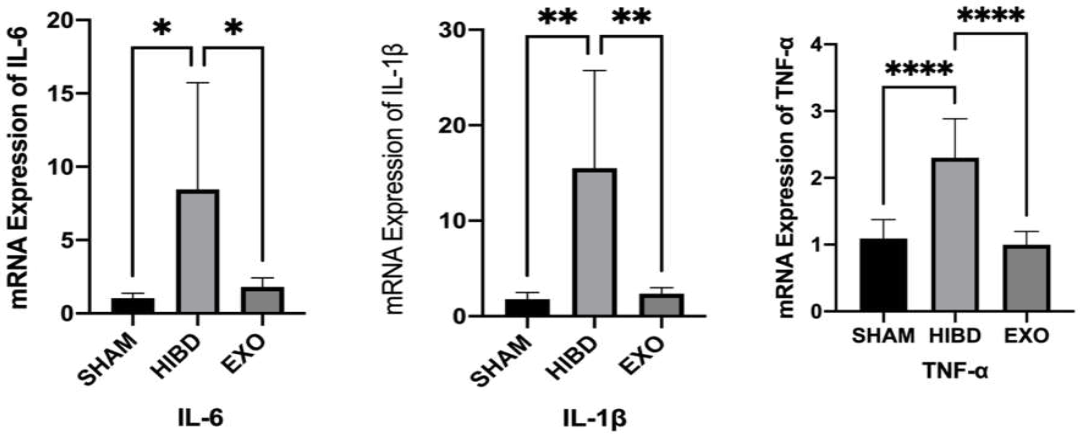


Figure 10. Down-regulation of inflammatory factors after EXOS transplantation in rats. mRNA expression levels of IL-6, IL-1β, and TNF-α in brain tissue from SHAM, HIBD, and EXOS groups measured by qPCR. Data are presented as mean ± SD from three independent experiments with three replicates. n=6, *$p < 0.05$、**$p < 0.01$、***$p < 0.001$.

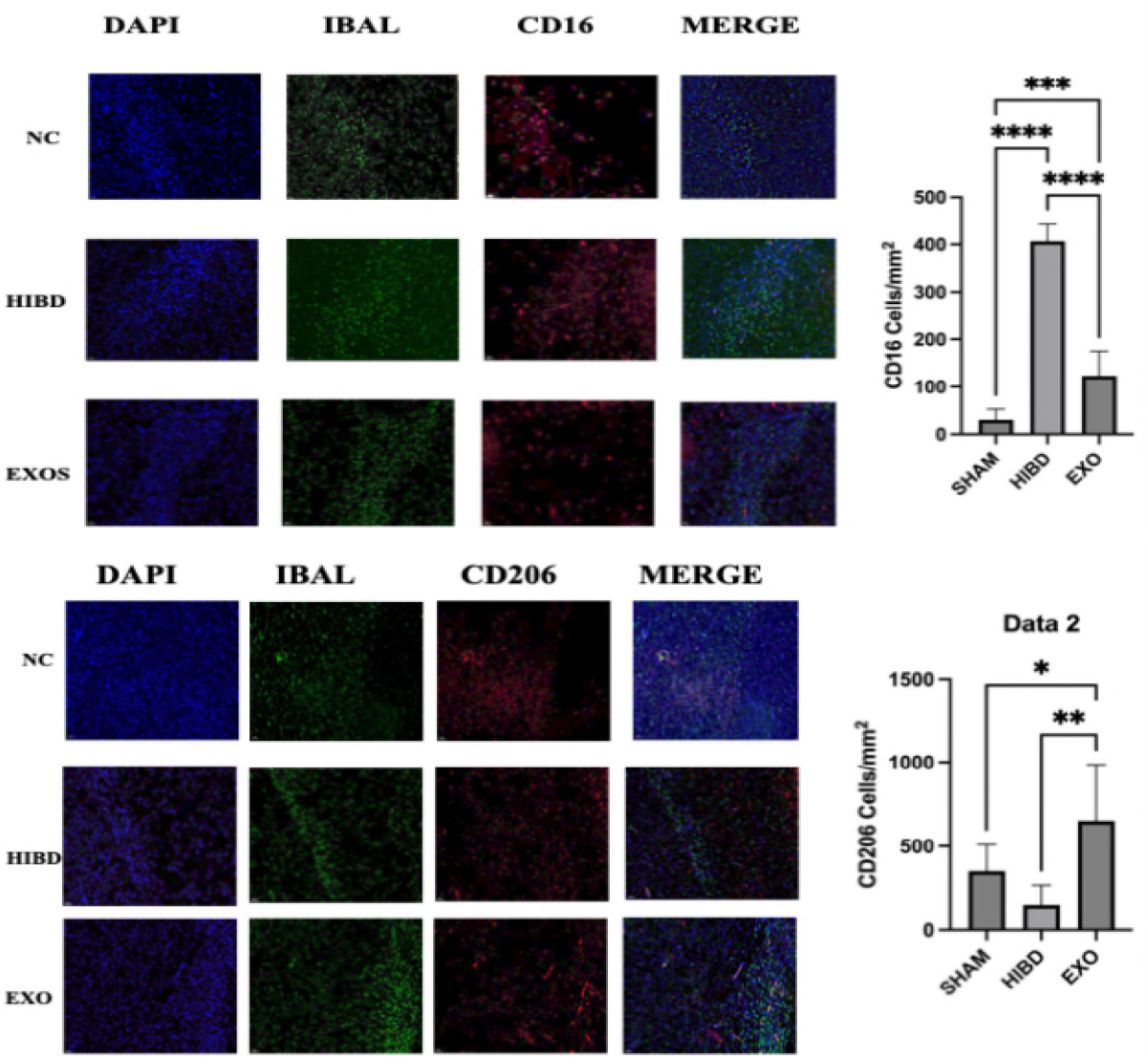


Figure 11. Immunofluorescence for CD16 and CD206 in brain tissue. Representative immunofluorescence images showing co-staining of microglial marker Iba1 with M1 marker CD16 and M2 marker CD206 in brain sections from SHAM, HIBD, and EXOS groups. Nuclei were counterstained with DAPI. Scale bar = 50 μm. n=3. *$p < 0.05$、**$p < 0.01$、***$p < 0.001$

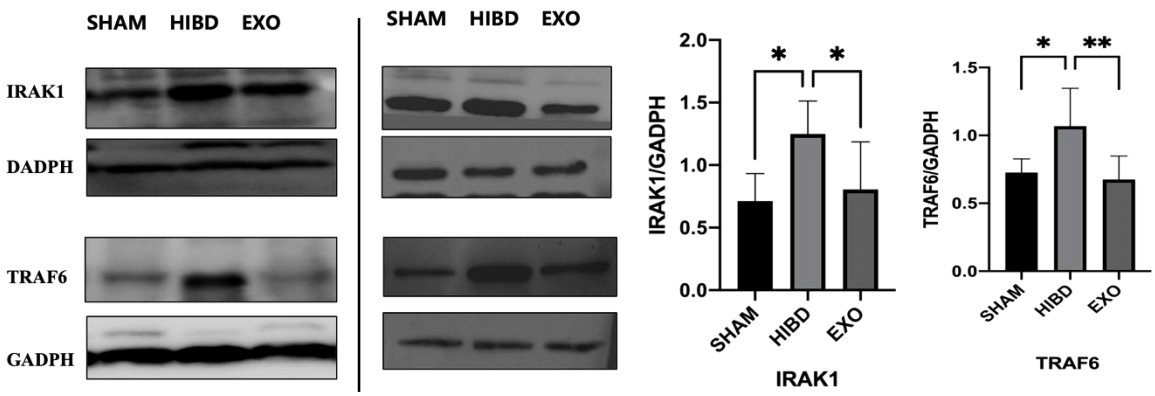


Figure 12. Expression of upstream inflammatory factor proteins in signaling pathway. Western blot analysis of IRAK1 and TRAF6 protein expression in brain tissue from SHAM, HIBD, and EXOS groups. Data are presented as mean ± SD, n=6. Black lines separate the two independent replicate blot shown in the same panel.*p <*0.05*、 **p < *0.01*、 ***p < *0.001*.

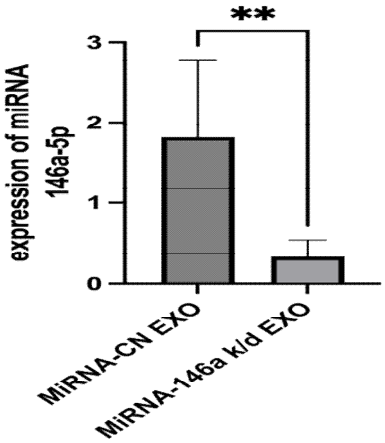


Figure 13. Assessing the efficiency of knocking down miRNA-146a-5p. qPCR analysis of miRNA-146a-5p expression in UC-MSC-EXOS following siRNA-mediated knockdown. Data are presented as mean ± SD, n=3. **p < 0.01.

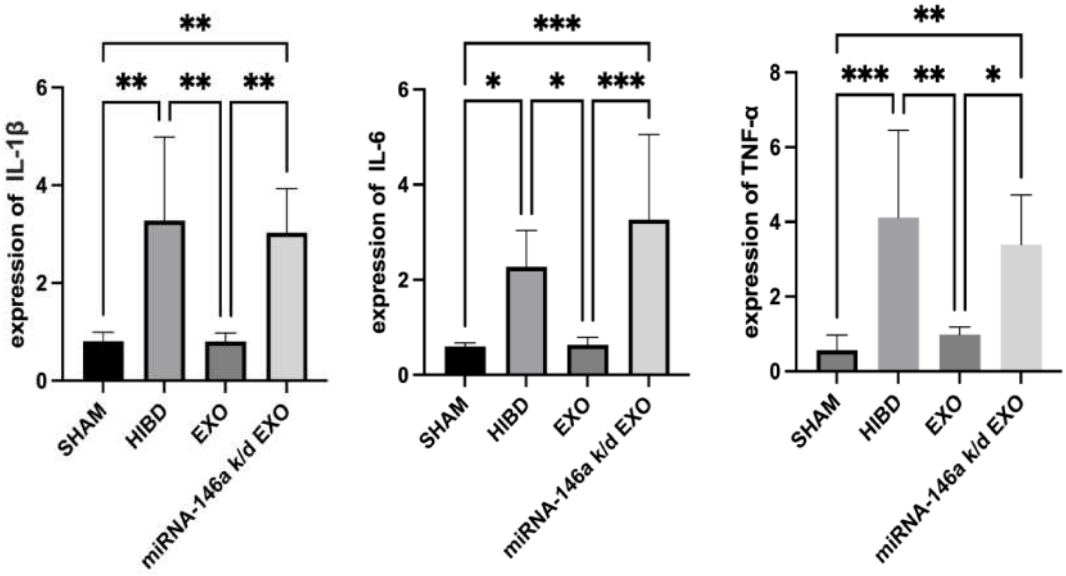


Figure 14. Inflammatory factors in brain tissue of rats with miRNA-146a-5p knockdown. mRNA expression levels of IL-6, IL-1β, and TNF-α in brain tissue from SHAM, HIBD, EXOS, and miRNA-146a k/d groups measured by qPCR. Data are presented as mean ± SD, n=6. *$p < 0.05$、**$p < 0.01$、***$p < 0.001$.

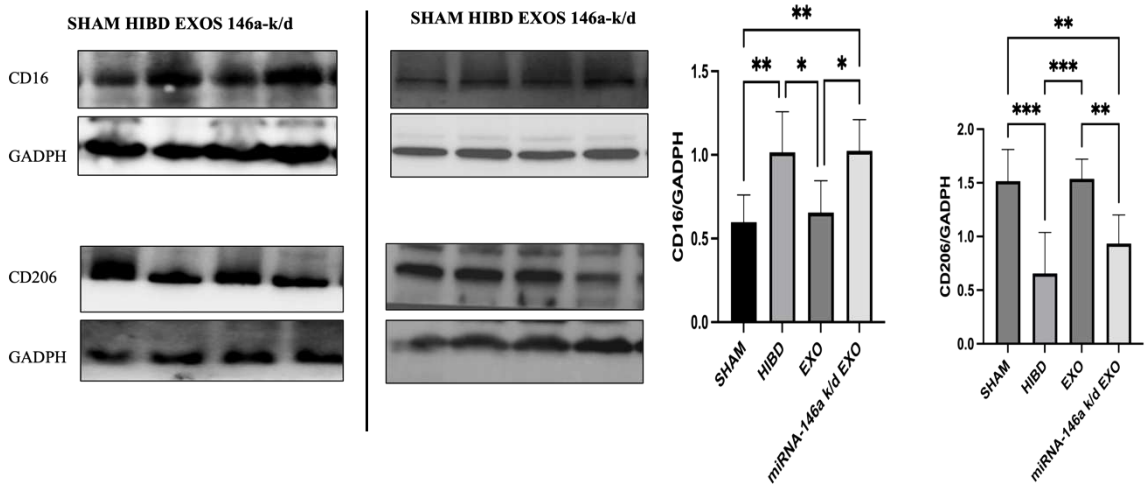


Figure 15A. Western blot analysis of M1 (CD16) and M2 (CD206) after miRNA-146a knockdown. Representative Western blot images and quantitative analysis of CD16 and CD206 protein expression in brain tissue from SHAM, HIBD, EXOS, and miRNA-146a k/d groups. Data are presented as mean ± SD, n=6. Black lines separate the two independent replicate blot shown in the same panel.*$P < 0.05$, **$P < 0.01$, ***$P < 0.001$.

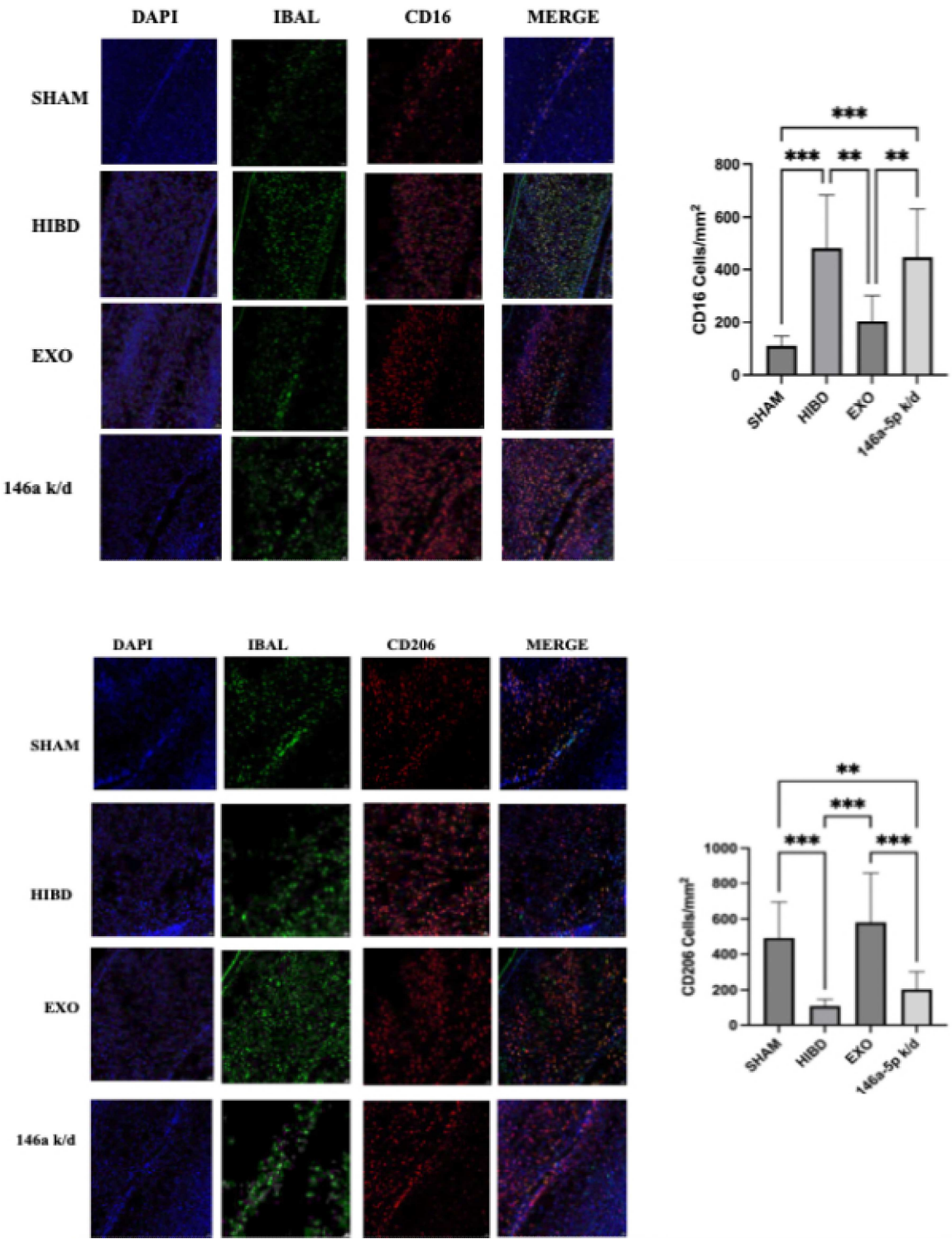


Figure 15B. Representative immunofluorescence images showing co-staining of Iba1 with CD16 and CD206 in brain sections from all groups. Scale bar = 50 μm, n=3. *$p < 0.05$、**$p < 0.01$、***$p < 0.001$.

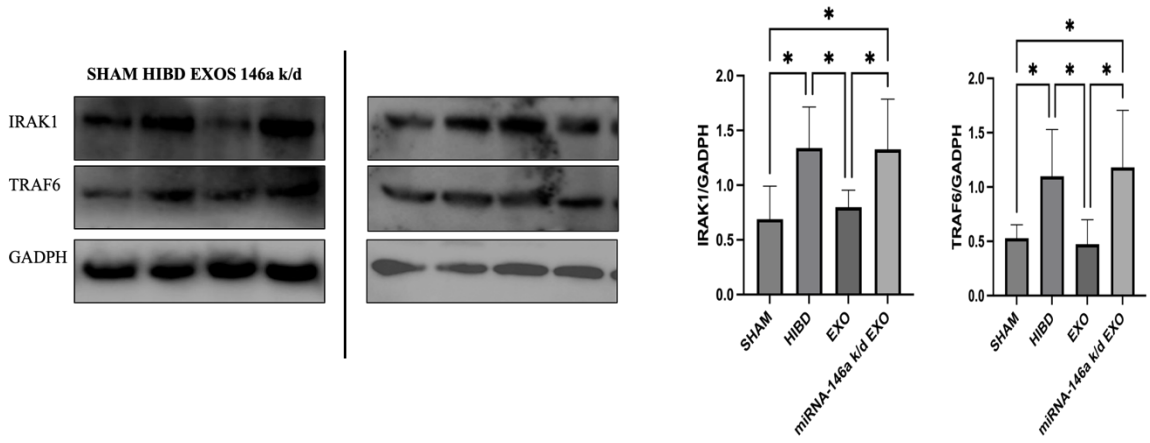


Figure 16. Western blot analysis of inflammatory factors upstream proteins after miRNA-146a knockdown in EXOS. Representative Western blot images and quantitative analysis of IRAK1 and TRAF6 protein expression in brain tissue from SHAM, HIBD, EXOS, and miRNA-146a k/d groups. Data are presented as mean ± SD, n=6. The grouping of blots cropped from different parts of the same blots but from same fields.*$p < 0.05$、**$p < 0.01$、***$p < 0.001$.

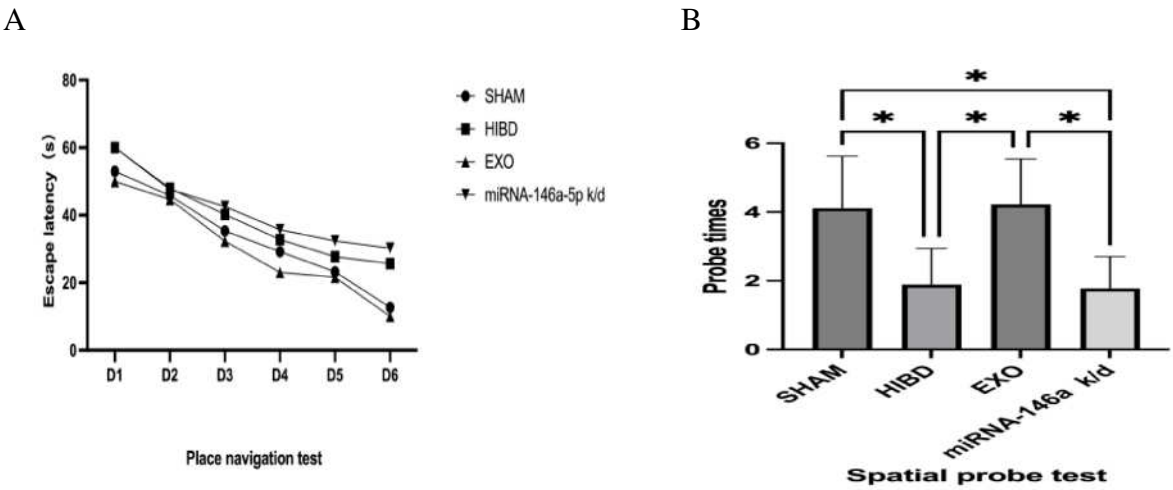


Figure 17. Escape latency and times of crossing the platform in the Morris water maze experiment. (A) Escape latency (time to reach hidden platform) over 5 consecutive training days for SHAM, HIBD, EXOS, and miRNA-146a k/d groups. (B) Number of platform crossings in the probe trial on day 6. Data are presented as mean ± SD, n=3. *$p < 0.05$

7. References

[1] J.J. Kurinczuk, M. White-Koning, and N. Badawi, Epidemiology of neonatal encephalopathy and hypoxic-ischaemic encephalopathy. Early Hum Dev 86 (2010) 329-338.

[2] J.E. Lawn, S. Cousens, and J. Zupan, 4 million neonatal deaths: when? Where? Why? Lancet 365 (2005) 891-900.

[3] M.K. Mwaniki, M. Atieno, J.E. Lawn, and C.R.J.C. Newton, Long-term neurodevelopmental outcomes after intrauterine and neonatal insults: a systematic review. Lancet 379 (2012) 445-452.

[4] P. Greco, G. Nencini, I. Piva, M. Scioscia, C.A. Volta, S. Spadaro, M. Neri, G. Bonaccorsi, F. Greco, I. Cocco, F. Sorrentino, F. D'Antonio, and L. Nappi, Pathophysiology of hypoxic-ischemic encephalopathy: a review of the past and a view on the future. Acta Neurol Belg 120 (2020) 277-288.

[5] E. Keleş, H.H. Kazan, A. Aral, and H. Bolay, Microglial iron trafficking: new player in brain injury. Turk J Med Sci 52 (2022) 1415-1424.

[6] U. Fisch, C. Brégère, F. Geier, L. Chicha, and R. Guzman, Neonatal hypoxia-ischemia in rat elicits a region-specific neurotrophic response in SVZ microglia. J Neuroinflammation 17 (2020) 26.

[7] H. Xue, Y.-H. Zhang, Q.-S. Gao, Z.-Y. Wu, J.-Y. Niu, C. Li, and P. Zhao, Sevoflurane Post-Conditioning Ameliorates Neuronal Deficits and Axon Demyelination After Neonatal Hypoxic Ischemic Brain Injury: Role of Microglia/Macrophage. Cell Mol Neurobiol 41 (2021) 1801-1816.

[8] C. Brégère, B. Schwendele, B. Radanovic, and R. Guzman, Microglia and Stem-Cell Mediated Neuroprotection after Neonatal Hypoxia-Ischemia. Stem Cell Rev Rep 18 (2022) 474-522.

[9] S. Guo, H. Wang, and Y. Yin, Microglia Polarization From M1 to M2 in Neurodegenerative Diseases. Front Aging Neurosci 14 (2022) 815347.

[10] B. Li, C. Dasgupta, L. Huang, X. Meng, and L. Zhang, MiRNA-210 induces microglial activation and regulates microglia-mediated neuroinflammation in neonatal hypoxic-ischemic encephalopathy. Cell Mol Immunol 17 (2020) 976-991.

[11] H. Ke, D. Liu, T. Li, X. Chu, D. Xin, M. Han, S. Wang, and Z. Wang, Hydrogen-Rich Saline Regulates Microglial Phagocytosis and Restores Behavioral Deficits Following Hypoxia-Ischemia Injury in Neonatal Mice via the Akt Pathway. Drug Des Devel Ther 14 (2020) 3827-3839.

[12] D. Xin, T. Li, X. Chu, H. Ke, D. Liu, and Z. Wang, MSCs-extracellular vesicles attenuated neuroinflammation, synapse damage and microglial phagocytosis after hypoxia-ischemia injury by preventing osteopontin expression. Pharmacol Res 164 (2021) 105322.

[13] M. Douglas-Escobar, and M.D. Weiss, Hypoxic-ischemic encephalopathy: a review for the clinician. JAMA Pediatr 169 (2015) 397-403.

[14] W. Walas, M. Wilińska, M. Bekiesińska-Figatowska, Z. Halaba, and R. Śmigiel, Methods for assessing the severity of perinatal asphyxia and early prognostic tools in neonates with hypoxic-ischemic encephalopathy treated with therapeutic hypothermia. Adv Clin Exp Med 29 (2020) 1011-1016.

[15] S.E. Jacobs, M. Berg, R. Hunt, W.O. Tarnow-Mordi, T.E. Inder, and P.G. Davis, Cooling for newborns with hypoxic ischaemic encephalopathy. Cochrane Database Syst Rev 2013 (2013) CD003311.

[16] P.W. Andrews, and N. Elvasorre, The origins of stem cells as tools for regenerative medicine. Biochem Biophys Res Commun 473 (2016) 663-664.

[17] N. Gurusamy, A. Alsayari, S. Rajasingh, and J. Rajasingh, Adult Stem Cells for Regenerative Therapy. Prog Mol Biol Transl Sci 160 (2018).

[18] M.M. Gabr, M.M. Zakaria, A.F. Refaie, A.M. Ismail, M.A. Abou-El-Mahasen, S.A. Ashamallah, S.M. Khater, S.M. El-Halawani, R.Y. Ibrahim, G.S. Uin, M. Kloc, R.Y. Calne, and M.A. Ghoneim, Insulin-

producing cells from adult human bone marrow mesenchymal stem cells control streptozotocin-induced diabetes in nude mice. Cell Transplant 22 (2013) 133-145.

[19] F.Y. Meligy, K. Shigemura, H.M. Behnsawy, M. Fujisawa, M. Kawabata, and T. Shirakawa, The efficiency of in vitro isolation and myogenic differentiation of MSCs derived from adipose connective tissue, bone marrow, and skeletal muscle tissue. In Vitro Cell Dev Biol Anim 48 (2012) 203-215.

[20] I.-S. Lee, K. Jung, M. Kim, and K.I. Park, Neural stem cells: properties and therapeutic potentials for hypoxic-ischemic brain injury in newborn infants. Pediatr Int 52 (2010) 855-865.

[21] P.M. Pimentel-Coelho, and R. Mendez-Otero, Cell therapy for neonatal hypoxic-ischemic encephalopathy. Stem Cells Dev 19 (2010) 299-310.

[22] P. Bianco, P.G. Robey, and P.J. Simmons, Mesenchymal stem cells: revisiting history, concepts, and assays. Cell Stem Cell 2 (2008) 313-319.

[23] M.H. Abumaree, F.M. Abomaray, M.A. Alshabibi, A.S. AlAskar, and B. Kalionis, Immunomodulatory properties of human placental mesenchymal stem/stromal cells. Placenta 59 (2017) 87-95.

[24] N.D. Theise, New principles of cell plasticity. C R Biol 325 (2002) 1039-1043.

[25] E.L. Herzog, L. Chai, and D.S. Krause, Plasticity of marrow-derived stem cells. Blood 102 (2003) 3483-3493.

[26] M.D. Hade, C.N. Suire, and Z. Suo, Mesenchymal Stem Cell-Derived Exosomes: Applications in Regenerative Medicine. Cells 10 (2021).

[27] A. Walewska, A. Janucik, M. Tynecka, M. Moniuszko, and A. Eljaszewicz, Mesenchymal stem cells under epigenetic control - the role of epigenetic machinery in fate decision and functional properties. Cell Death Dis 14 (2023) 720.

[28] A. Naji, M. Eitoku, B. Favier, F. Deschaseaux, N. Rouas-Freiss, and N. Suganuma, Biological functions of mesenchymal stem cells and clinical implications. Cell Mol Life Sci 76 (2019) 3323-3348.

[29] S. Koh, N. Kim, H.H. Yin, I.R. Harris, N.S. Dejneka, and C. Eroglu, Human Umbilical Tissue-Derived Cells Promote Synapse Formation and Neurite Outgrowth via Thrombospondin Family Proteins. J Neurosci 35 (2015) 15649-15665.

[30] C.M. Cotten, K. Fisher, W. Malcolm, K.E. Gustafson, L. Cheatham, A. Marion, R. Greenberg, and J. Kurtzberg, A Pilot Phase I Trial of Allogeneic Umbilical Cord Tissue-Derived Mesenchymal Stromal Cells in Neonates With Hypoxic-Ischemic Encephalopathy. Stem Cells Transl Med 12 (2023) 355-364.

[31] S.B. Powell, and J.M. Silvestri, Safety of Intratracheal Administration of Human Umbilical Cord Blood Derived Mesenchymal Stromal Cells in Extremely Low Birth Weight Preterm Infants. J Pediatr 210 (2019).

[32] S.Y. Ahn, Y.S. Chang, S.I. Sung, and W.S. Park, Mesenchymal Stem Cells for Severe Intraventricular Hemorrhage in Preterm Infants: Phase I Dose-Escalation Clinical Trial. Stem Cells Transl Med 7 (2018) 847-856.

[33] L.M. Doyle, and M.Z. Wang, Overview of Extracellular Vesicles, Their Origin, Composition, Purpose, and Methods for Exosome Isolation and Analysis. Cells 8 (2019).

[34] J. Zhang, S. Li, L. Li, M. Li, C. Guo, J. Yao, and S. Mi, Exosome and exosomal microRNA: trafficking, sorting, and function. Genomics Proteomics Bioinformatics 13 (2015) 17-24.

[35] Y. Yaghoubi, A. Movassaghpour, M. Zamani, M. Talebi, A. Mehdizadeh, and M. Yousefi, Human umbilical cord mesenchymal stem cells derived-exosomes in diseases treatment. Life Sci 233 (2019) 116733.

[36] F.J. Vizoso, N. Eiro, S. Cid, J. Schneider, and R. Perez-Fernandez, Mesenchymal Stem Cell Secretome: Toward Cell-Free Therapeutic Strategies in Regenerative Medicine. Int J Mol Sci 18 (2017).

[37] J.A. Ankrum, J.F. Ong, and J.M. Karp, Mesenchymal stem cells: immune evasive, not immune privileged. Nat Biotechnol 32 (2014) 252-260.

[38] D.R.M.G. Ophelders, T.G.A.M. Wolfs, R.K. Jellema, A. Zwanenburg, P. Andriessen, T. Delhaas, A.-K. Ludwig, S. Radtke, V. Peters, L. Janssen, B. Giebel, and B.W. Kramer, Mesenchymal Stromal Cell-Derived Extracellular Vesicles Protect the Fetal Brain After Hypoxia-Ischemia. Stem Cells Transl Med 5 (2016) 754-763.

[39] V. Börger, M. Bremer, R. Ferrer-Tur, L. Gockeln, O. Stambouli, A. Becic, and B. Giebel, Mesenchymal Stem/Stromal Cell-Derived Extracellular Vesicles and Their Potential as Novel Immunomodulatory Therapeutic Agents. Int J Mol Sci 18 (2017).

[40] L.C. Liew, T. Katsuda, L. Gailhouste, H. Nakagama, and T. Ochiya, Mesenchymal stem cell-derived extracellular vesicles: a glimmer of hope in treating Alzheimer's disease. Int Immunol 29 (2017) 11-19.

[41] J.W. Jung, M. Kwon, J.C. Choi, J.W. Shin, I.W. Park, B.W. Choi, and J.Y. Kim, Familial occurrence of pulmonary embolism after intravenous, adipose tissue-derived stem cell therapy. Yonsei Med J 54 (2013) 1293-1296.

[42] H. Abbaszadeh, F. Ghorbani, M. Derakhshani, A. Movassaghpour, and M. Yousefi, Human umbilical cord mesenchymal stem cell-derived extracellular vesicles: A novel therapeutic paradigm. J Cell Physiol 235 (2020) 706-717.

[43] S. Bruno, C. Grange, M.C. Deregibus, R.A. Calogero, S. Saviozzi, F. Collino, L. Morando, A. Busca, M. Falda, B. Bussolati, C. Tetta, and G. Camussi, Mesenchymal stem cell-derived microvesicles protect against acute tubular injury. J Am Soc Nephrol 20 (2009) 1053-1067.

[44] S. Gatti, S. Bruno, M.C. Deregibus, A. Sordi, V. Cantaluppi, C. Tetta, and G. Camussi, Microvesicles derived from human adult mesenchymal stem cells protect against ischaemia-reperfusion-induced acute and chronic kidney injury. Nephrol Dial Transplant 26 (2011) 1474-1483.

[45] Y. Zhang, M. Chopp, Y. Meng, M. Katakowski, H. Xin, A. Mahmood, and Y. Xiong, Effect of exosomes derived from multipluripotent mesenchymal stromal cells on functional recovery and neurovascular plasticity in rats after traumatic brain injury. J Neurosurg 122 (2015) 856-867.

[46] Z. Wang, F. Liu, M. Wei, Y. Qiu, C. Ma, L. Shen, and Y. Huang, Chronic constriction injury-induced microRNA-146a-5p alleviates neuropathic pain through suppression of IRAK1/TRAF6 signaling pathway. J Neuroinflammation 15 (2018) 179.

[47] J. Hou, Q. Deng, X. Deng, W. Zhong, S. Liu, and Z. Zhong, MicroRNA-146a-5p alleviates lipopolysaccharide-induced NLRP3 inflammasome injury and pro-inflammatory cytokine production via the regulation of TRAF6 and IRAK1 in human umbilical vein endothelial cells (HUVECs). Ann Transl Med 9 (2021) 1433.

[48] R. Aquino, V. de Concini, M. Dhenain, S. Lam, D. Gosset, L. Baquedano, M.G. Forero, A. Menuet, P. Baril, and C. Pichon, Intrahippocampal Inoculation of Aβ1-42 Peptide in Rat as a Model of Alzheimer's Disease Identified MicroRNA-146a-5p as Blood Marker with Anti-Inflammatory Function in Astrocyte Cells. Cells 12 (2023).

[49] I. Gilyazova, D. Asadullina, E. Kagirova, R. Sikka, A. Mustafin, E. Ivanova, K. Bakhtiyarova, G. Gilyazova, S. Gupta, E. Khusnutdinova, H. Gupta, and V. Pavlov, MiRNA-146a-A Key Player in Immunity and Diseases. Int J Mol Sci 24 (2023).

[50] A.E. Williams, M.M. Perry, S.A. Moschos, H.M. Larner-Svensson, and M.A. Lindsay, Role of miRNA-

146a in the regulation of the innate immune response and cancer. Biochem Soc Trans 36 (2008) 1211-1215.
[51] Y.-C. Chang, and C.-C. Huang, Perinatal brain injury and regulation of transcription. Curr Opin Neurol 19 (2006) 141-147.
[52] C. Thery, S. Amigorena, G. Raposo, and A. Clayton, Isolation and characterization of exosomes from cell culture supernatants and biological fluids. Current protocols in cell biology Chapter 3 (2006) Unit 3 22.
[53] M. Zhao, P. Zhu, M. Fujino, J. Zhuang, H. Guo, I. Sheikh, L. Zhao, and X.-K. Li, Oxidative Stress in Hypoxic-Ischemic Encephalopathy: Molecular Mechanisms and Therapeutic Strategies. Int J Mol Sci 17 (2016).
[54] H. Quan, and R. Zhang, Microglia dynamic response and phenotype heterogeneity in neural regeneration following hypoxic-ischemic brain injury. Front Immunol 14 (2023) 1320271.
[55] Y.S. Chang, S.Y. Ahn, H.S. Yoo, S.I. Sung, S.J. Choi, W.I. Oh, and W.S. Park, Mesenchymal stem cells for bronchopulmonary dysplasia: phase 1 dose-escalation clinical trial. J Pediatr 164 (2014).
[56] S.Y. Ahn, Y.S. Chang, J.H. Kim, S.I. Sung, and W.S. Park, Two-Year Follow-Up Outcomes of Premature Infants Enrolled in the Phase I Trial of Mesenchymal Stem Cells Transplantation for Bronchopulmonary Dysplasia. J Pediatr 185 (2017).
[57] D.J. Prockop, The exciting prospects of new therapies with mesenchymal stromal cells. Cytotherapy 19 (2017) 1-8.
[58] S.Y. Ahn, Y.S. Chang, D.K. Sung, S.I. Sung, J.-Y. Ahn, and W.S. Park, Pivotal Role of Brain-Derived Neurotrophic Factor Secreted by Mesenchymal Stem Cells in Severe Intraventricular Hemorrhage in Newborn Rats. Cell Transplant 26 (2017) 145-156.
[59] S.Y. Ahn, W.S. Park, Y.E. Kim, D.K. Sung, S.I. Sung, J.Y. Ahn, and Y.S. Chang, Vascular endothelial growth factor mediates the therapeutic efficacy of mesenchymal stem cell-derived extracellular vesicles against neonatal hyperoxic lung injury. Exp Mol Med 50 (2018).
[60] Y. Chen, Y. Tang, W. Long, and C. Zhang, Stem Cell-Released Microvesicles and Exosomes as Novel Biomarkers and Treatments of Diseases. Stem Cells International 2016 (2016) 2417268.
[61] T. Zhou, C. He, P. Lai, Z. Yang, Y. Liu, H. Xu, X. Lin, B. Ni, R. Ju, W. Yi, L. Liang, D. Pei, C.E. Egwuagu, and X. Liu, miR-204-containing exosomes ameliorate GVHD-associated dry eye disease. Sci Adv 8 (2022) eabj9617.
[62] J. Zhao, X. Li, J. Hu, F. Chen, S. Qiao, X. Sun, L. Gao, J. Xie, and B. Xu, Mesenchymal stromal cell-derived exosomes attenuate myocardial ischaemia-reperfusion injury through miR-182-regulated macrophage polarization. Cardiovasc Res 115 (2019) 1205-1216.
[63] P. Xian, Y. Hei, R. Wang, T. Wang, J. Yang, J. Li, Z. Di, Z. Liu, A. Baskys, W. Liu, S. Wu, and Q. Long, Mesenchymal stem cell-derived exosomes as a nanotherapeutic agent for amelioration of inflammation-induced astrocyte alterations in mice. Theranostics 9 (2019) 5956-5975.
[64] C. Ju, Y. Li, Y. Shen, Y. Liu, J. Cai, N. Liu, G. Ma, and Y. Tang, Transplantation of Cardiac Mesenchymal Stem Cell-Derived Exosomes for Angiogenesis. J Cardiovasc Transl Res 11 (2018) 429-437.
[65] C. Fan, Y. Li, T. Lan, W. Wang, Y. Long, and S.Y. Yu, Microglia secrete miR-146a-5p-containing exosomes to regulate neurogenesis in depression. Mol Ther 30 (2022) 1300-1314.
[66] T. Hua, M. Yang, H. Song, E. Kong, M. Deng, Y. Li, J. Li, Z. Liu, H. Fu, Y. Wang, and H. Yuan, Huc-MSCs-derived exosomes attenuate inflammatory pain by regulating microglia pyroptosis and autophagy via the miR-146a-5p/TRAF6 axis. J Nanobiotechnology 20 (2022) 324.
[67] X. Chen, W. Li, T. Chen, X. Ren, J. Zhu, F. Hu, J. Luo, L. Xing, H. Zhou, J. Sun, Q. Jiang, Y. Zhang, and

Q. Xi, miR-146a-5p promotes epithelium regeneration against LPS-induced inflammatory injury via targeting TAB1/TAK1/NF-κB signaling pathway. Int J Biol Macromol 221 (2022) 1031-1040.

[68] L.-C. Su, W.-D. Xu, and A.-F. Huang, IRAK family in inflammatory autoimmune diseases. Autoimmun Rev 19 (2020) 102461.

[69] J.W. Singer, A. Fleischman, S. Al-Fayoumi, J.O. Mascarenhas, Q. Yu, and A. Agarwal, Inhibition of interleukin-1 receptor-associated kinase 1 (IRAK1) as a therapeutic strategy. Oncotarget 9 (2018) 33416-33439.

[70] T. Liu, D.-M. Wu, F. Zhang, T. Zhang, M. He, Y.-Y. Zhao, J. Li, L. Li, and Y. Xu, miR-142a-3p Enhances FlaA N/C Protection Against Radiation-Mediated Intestinal Injury by Modulating the IRAK1/NF-κB Signaling Pathway. Int J Radiat Oncol Biol Phys 112 (2022) 1256-1268.

[71] D.-F. Meng, R. Sun, G.-Y. Liu, L.-X. Peng, L.-S. Zheng, P. Xie, S.-T. Lin, Y. Mei, Y.-Y. Qiang, C.-Z. Li, L. Xu, X.-S. Peng, H. Hu, Y.-H. Lang, Z.-J. Liu, M.-D. Wang, L.-L. Guo, D.-H. Xie, D.-T. Shu, H.-F. Li, F.-F. Luo, X.-T. Niu, B.-J. Huang, and C.-N. Qian, S100A14 suppresses metastasis of nasopharyngeal carcinoma by inhibition of NF-kB signaling through degradation of IRAK1. Oncogene 39 (2020) 5307-5322.

[72] H.S. Kwon, and S.-H. Koh, Neuroinflammation in neurodegenerative disorders: the roles of microglia and astrocytes. Transl Neurodegener 9 (2020) 42.

[73] L.-R. Liu, J.-C. Liu, J.-S. Bao, Q.-Q. Bai, and G.-Q. Wang, Interaction of Microglia and Astrocytes in the Neurovascular Unit. Front Immunol 11 (2020) 1024.

[74] C.-T. Jiang, W.-F. Wu, Y.-H. Deng, and J.-W. Ge, Modulators of microglia activation and polarization in ischemic stroke (Review). Mol Med Rep 21 (2020) 2006-2018.

Supplementary Files

This is a list of supplementary files associated with this preprint. Click to download.

- F11.zip
- F15B.zip
- Morriswatermazeexperiment.zip
- Supplementarymaterialsoforiginaldata2.xlsx
- Supplementarymaterialsoforiginaldata260530.docx